Particle bursts from thunderclouds: Natural particle accelerators above our heads

Ashot Chilingarian,* Gagik Hovsepyan, and Armen Hovhannisyan
Artem Alikhanyan National Laboratory, Alikhanyan Brothers 2, Yerevan – 36, Armenia
(Received 13 November 2010; published 1 March 2011)

Strong electrical fields inside thunderclouds give rise to fluxes of high-energy electrons and, consequently, gamma rays and neutrons. Gamma rays and electrons are currently detected by the facilities of low orbiting satellites and by networks of surface particle detectors. During intensive particle fluxes, coinciding with thunderstorms, series of particle bursts were detected by the particle detectors of Aragats Space Environmental Center at an altitude of 3250 m. We classify the thunderstorm ground enhancements in 2 categories, one lasting microseconds, and the other lasting tens of minutes. Both types of events can occur at the same time, coinciding with a large negative electric field between the cloud and the ground and negative intracloud lightning. Statistical analysis of the short thunderstorm ground enhancement bursts sample suggests the duration is less than 50 μs and spatial extension is larger than 1000 m^2. We discuss the origin of thunderstorm ground enhancements and its connection to the terrestrial gamma flashes detected by orbiting gamma-ray observatories.

DOI: 10.1103/PhysRevD.83.062001 PACS numbers: 92.60.Pw, 13.40.−f, 94.05.Dd

I. INTRODUCTION

High-energy particles and radiation of an atmospheric nature is registered in space and on the Earth's surface. Terrestrial gamma-ray flashes (TGFs)—brief bursts of gamma rays[1] produced in the atmosphere—have been firmly established during the last decades by the gamma-ray observatories aboard low-Earth orbit satellites [2–5]. It is generally accepted that the gamma rays in TGFs come from the bremsstrahlung radiation of energetic electrons. Inside thunderclouds, the electric fields can grow large enough to force fast electrons to gain energy from the field larger than the braking force and ''run away.'' As the runaway electrons travel through air, they undergo hard elastic scattering with atomic electrons, producing additional electrons that can also run away. In this way the electrical fields in the thunderstorm atmospheres give the ambient population of the MeV electrons from the cosmic-ray showers a boost by increasing the number of energetic particles through a multiplication and acceleration process called relativistic runaway electron avalanche (RREA) [6,7]. The source of TGFs is located in the space just above or even within thunderclouds (12–20 km above Earth's surface; see [1]). The RREA mechanism can create large amounts of high-energy electrons and subsequently the gamma rays. The nature of seed particles is still under debate; an alternative source of the seed particles could be connected with the lightning step leaders [8–10]. As we will demonstrate in this paper, the very short time span of the discovered thunderstorm ground enhancement (TGE) events supports their lightning origin. However, it is possible that some other mechanisms are responsible for the high-energy phenomena in thunderclouds. Until now there were surprisingly few observations on the electric field dynamics in the thunderstorm atmospheres.

The amount of the surface detection of the electron and gamma-ray fluxes correlated with thunderstorms is not too large (see the review in [11]). Only at the Baksan Neutrino Observatory of the Institute for Nuclear Research [12] and at the Tien-Shan Cosmic Ray Station of the Lebedev Institute, both Russian Academy of Sciences, have surface particle enhancements correlated with thunderstorms been studied for many years in a systematic way. Unfortunately, the location of the surface array in the Baksan valley did not allow registration of large fluxes. The array is located in a deep narrow valley, and thunderclouds are rather high. The Tien-Shan group has concentrated mostly on the research of the very rare process—runaway breakdown initiated by an extensive air shower (EAS) with energy above 1000 TeV, so-called runaway breakdown-EAS discharge [6].

However, if electron and gamma-ray fluxes are unambiguously detected by orbiting gamma-ray observatories ~500 km from the source, we can expect the intensive particle and radiation fluxes on the highland altitudes from thunderclouds located a few hundred meters above. The particle detectors of the Aragats Space Environment Center (ASEC) [13,14] continuously measure the time series of the charged and neutral fluxes of the secondary cosmic rays. ASEC detectors measure 1 min and 10 sec time series starting from the minimal energy of 3 until 250 MeV, as well as time series of numbers of the EASs initiated in the atmosphere by primary protons or stripped nuclei with energy greater than ~50 TeV. Numerous thunderstorm correlated enhancements of electrons, gamma rays, and neutrons, detected by the ASEC facilities at the minimum of the solar activity years, constitute a rich

*chili@aragats.am
[1]Recently, Ref. [1] reported that a substantial fraction of TGF events are not gamma rays but high-energy electrons; see also [2].

experimental set to investigate the high-energy phenomena in the thunderstorm atmospheres. The Aragats High-Mountain Research Station of the Artem Alikhanyan National Laboratory (former Yerevan Physics Institute) is located 3250 m above sea level near the southern peak of Aragats (3750 m above sea level); the other 3 peaks of Aragats are located from 10 to 15 km away. The thunderstorm activity on Aragats is strongest in May–June and September–October. Thunderclouds are usually below the southern peak and sometimes 100–200 m only above the station. In 2009–2010 we measured several long TGEs of tens of minutes duration. During the two most intense of these, on 19 September, 2009 and 4 October, 2010, the Maket surface array [15] also detected a series of electron/gamma-ray bursts—short TGEs—extended showers of the coherent particles simultaneously detected in the scintillators of the surface array within a time window of 1 μs. In this paper, we discuss the short TGEs detection by the surface facilities and its relation to the TGFs detected by satellite facilities. We will demonstrate that TGEs have a duration not greater than 50 μs and will discuss their origin.

II. DETECTION OF THE THUNDERSTORM CORRELATED COSMIC-RAY BURSTS ON 4 OCTOBER, 2010

Most of the ASEC particle detectors and field meters are located in the Maket building (see Fig. 1) and nearby. Along with 16 plastic scintillators belonging to the Maket surface array, in operation are the Aragats Solar Neutron Telescope (ASNT), the Aragats neutron monitor of type 18NM64, and the Space Environmental Viewing and Analysis Network (SEVAN) particle detectors

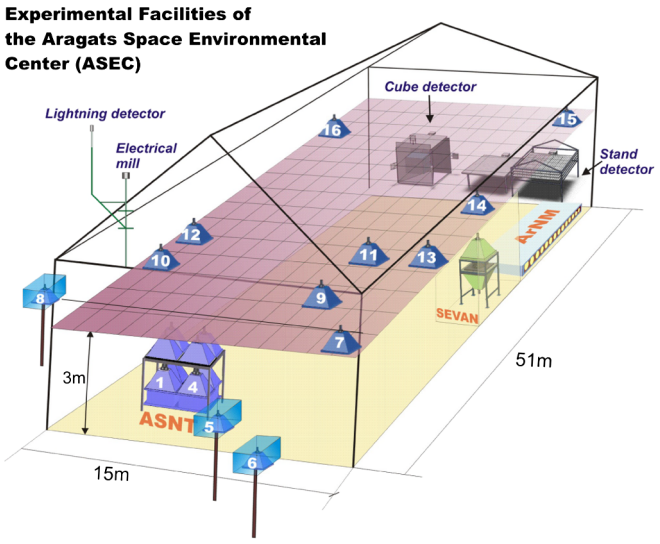

FIG. 1 (color online). Particle detectors and field meters of the Aragats Space Environmental Center operation during the 2010 measurement campaign.

(see the detailed description in [11]). In 2010, especially for the detection of low-energy electrons and gamma rays from thunderclouds, two new outdoor facilities were installed near the Maket building, namely, the Stand and Cube scintillation detectors. The Stand detector is a 3-layered pile of 1 cm thick and 1 m^2 area molded plastic scintillators with fiberglass wavelength shifters, fabricated by the High Energy Physics Institute, Serpukhov, Russian Federation. The same type of 3 cm thick scintillator is located also outdoors. The energy thresholds of the 1 cm thick scintillators are ~2, 6, and 10 MeV correspondingly from the top to the bottom: The energy threshold of the 3 cm thick scintillator is ~5 MeV. The energy thresholds of the rest of the ASEC scintillators range from 7 to 18 MeV (dependent on the amount of matter above); therefore in 2009 we reconstructed the energy spectra of RREA electrons and gamma rays starting from 7 MeV. The energy spectra of the 2010 campaign were reconstructed starting from 2 MeV. The aim of the Cube detector is to measure both charged and neutral fluxes separately, with enhanced purity of the neutral flux. For it the assembly of two 20 cm thick and 0.25 m^2 area plastic scintillators is fully surrounded by six 1 cm thick 1 m^2 area plastic scintillators, forming the veto for charged particles to enter the sensitive volume and hit the thick scintillators. The detector measures count rates of the neutral particles if there is at least one signal from the two inner scintillators without any signal from the surrounding veto scintillators. The histograms of the energy deposits in the two inner thick scintillators are stored every minute. The one-minute count rates of the surrounding 6 scintillators are measured and stored as well.

In 2010 we installed in the Maket building the magnetotelluric station LEMI-417, designed and commissioned by Lviv Center of the Space Research Institute of Ukrainian Academy of Science. One-second time series of the three-dimensional measurement of the geomagnetic field enter the ASEC database, which will highly improve the research of correlations of the geomagnetic parameters and changes of the fluxes of cosmic rays. The same device is measuring also components of the electric field. Additionally, on the roof of the building we installed an electrical field mill for measuring electrical fields between clouds and the ground and a lightning detector, measuring the broadband radio emissions by the intracloud, intercloud, and cloud-ground lightning (see Figs. 1 and 10).

In 2009–2010 we detected simultaneously large fluxes of electrons, gamma rays, and neutrons correlated with thunderstorm activity [11]. During the period of the count rate enhancements lasting tens of minutes, millions of additional particles were detected (see the appendix for discussion on the possible interferences with electronic or natural induced signals).

On October 4, 2010, all ASEC particle detectors measured a large enhancement of count rates seen as huge

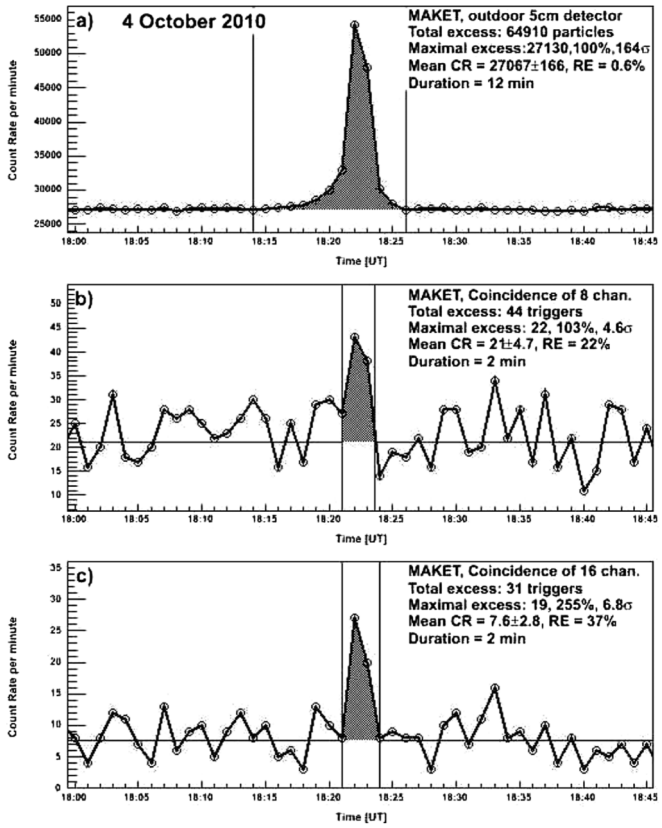

FIG. 2. One-minute time series detected by the Maket array. (a) Count rate of the standalone outer detector (energy threshold ~7 MeV); (b) count rates of the ''EAS hardware trigger''—9 scintillators give a signal within 1 μs); (c) count rate of the EAS software triggers—off-line selection of events where all 16 scintillators give a signal within 1 μs.

peaks in the time series (see Fig. 2). In the legend of Fig. 2, we depict a total enhancement during the event, the maximal enhancement that occurred during 1 min, and the statistical significance of the detected peak in percents and numbers of standard deviations (σ). The mean count rate (CR), the variance, and the relative error (RE) of the time series were estimated by the 1-hour data before the start of enhancement when the mean and variance of the count rate correspond to the detector typical operation.[2] In Fig. 2(a), one can see the huge enhancement of the count rate measured by the outdoor scintillator of the Maket array (energy threshold 7 MeV) with maximal enhancement at 18:23 (100%, 164σ). In the time series of the number of the Maket hardware triggers (as minimum 9 ''fired'' scintillators), the maximal enhancement of the count rate can be seen during the same minute [Fig. 2(b)]—the peak of ~103% magnitude and ~4.6σ significance.[3] When we apply software trigger and select events with all 16 scintillators fired, this enhancement magnifies up to ~250% and ~7σ [Fig. 2(c)]. It is indirect evidence that the TGE events cover much larger space than ''background''[4] EAS events (we will discuss the size of the EAS and TGE events in more detail in the following section).

III. CLASSIFICATION OF THE EAS AND TGE EVENTS

Based on the expected systematic difference of the EAS and TGE event densities, we perform a two-way classification of showers detected on 19 September and 4 October, 2010[5] We select the 10-minute sample of the pure background—EAS events measured during quiet weather. Having 2 samples, one containing the pure background and the other a signal contaminated by background, we can pose the problem of the signal ''purification,'' i.e. selecting the decision boundary in the measured parameter space and performing cuts of the experimental sample containing signal and background. The boundary in the space of measured characteristics (decision boundary) should be optimized in such a way as to keep as many as possible of the signal events and suppress as many as possible of the background events. Obviously, we cannot keep 100% of the signal and reject all background events, because of the overlapping signal and background distributions; therefore, we have to select a compromise. The typical particle density distribution of the EAS hitting Earth's surface is a bell-like two-dimensional distribution with a large fraction of the shower particles near the core of EAS. The TGE event that originated from multiple avalanches of electrons with maximal energy not exceeding 50 MeV [11] is expected to be uniform without any significant particle density peaks.

Almost all of the additional Maket triggers [Figs. 2(b) and 2(c)] have mean density not exceeding 7–8 particles/m^2, and we can restrict ourselves by the one-dimensional classification scheme, using only the mean density of an event. However, as we can see in Fig. 3, to the right from the decision line in the region of low density there is a population of events with rather large maximal density. We treat these events as background small EAS events with their shower axes fallen in the array.

[2]Mean count rates and variances of the ASEC particle detectors were very stable in 2009–2010 due to continuous maintenance and the absence of the solar modulation effects during an unusual long period of a quiet Sun.

[3]The coherent short bursts of the thunderstorm correlated particle fluxes were first detected during the event of 19 September, 2009 (see details in [11]).

[4]The background for the triggered events is extensive air showers routinely generated by primary protons or stripped nuclei entering the atmosphere. Comparing the mean background count rate with the intensity of the primary cosmic rays, we estimate the threshold energy of the primary proton flux detected by the Maket array to be 50–100 TeV.

[5]We form a joint sample of events (total 613) containing background—EAS—and ''signal''—TGE—events.

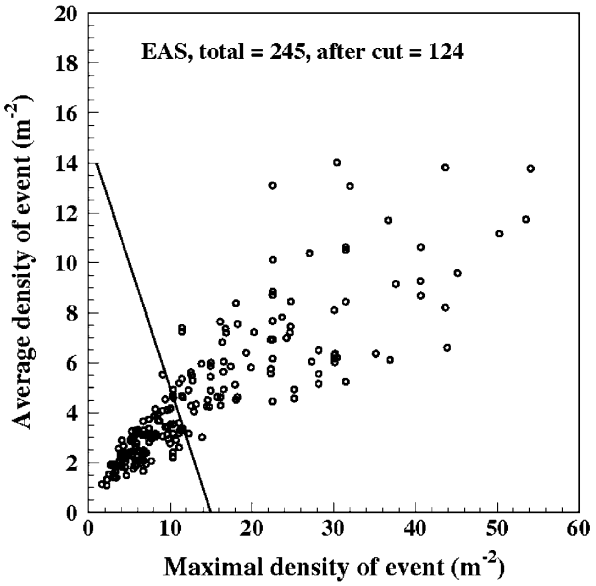

FIG. 3. Scatter plot of the registered at quiet weather Maket triggers; pure EAS events.

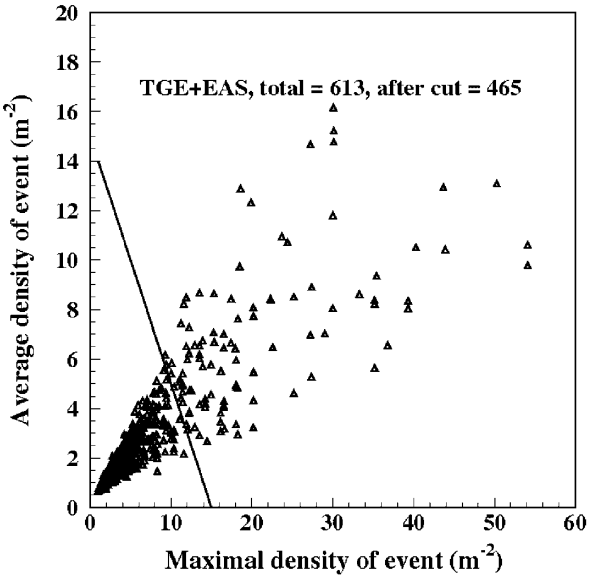

FIG. 4. Two-way classification of the showers detected on 19 September, 2009, and 4 October, 2010, during thunderstorms.

To additionally suppress such events we add the second discriminator—the maximal density within an event. Thus, the mean and maximal densities of Maket scintillators that detected the shower were used for classification. The selection procedure is visualized in Figs. 3 and 4. The showers with parameters in the region to the left from the linear decision boundary are classified as TGE events and the events to the right as EAS events.

Selected classification criteria suppress ~50% of the EAS events (121 from 245; see Fig. 3) but only losing ~25% of the joint EAS and TGE events (148 from 613; Fig. 4). Among the selected 465 signal events we expect about 121 background events; therefore, the expected purity of the selected TGE sample is rather high: ~75%. The 25% of contamination could not be significantly reduced due to large EAS with axes far from the Maket array. The long tails of EASs generate events with low mean and maximal densities and could not be distinguished from TGEs.

Further evidence of the difference of the two classes of events is apparent from Fig. 5. The density distribution of EAS events follows a power law as many other distributions generically connected with population of the galactic cosmic rays falling on the atmosphere. In contrast, the density distribution of the TGE events (obtained by subtraction of the pure EAS sample from the joint TGE + EAS sample) follows an exponential curve, as expected from an avalanche process. The average value of the mean density of EAS and TGE classes is ~6 and 2.5 particles/m^2, correspondingly. The density spectra of the TGE + EAS and pure EAS events are drastically different in the region of small densities (less than 7–8 particles/m^2) and identical for higher densities.

The comparison of the spatial extension of both classes is shown in Fig. 6. All 16 Maket array scintillators used for the detection of particle showers are located on the area of ~1000 m^2.

If in the off-line analysis we require more than 9 scintillators (hardware trigger condition) to be fired, the number of events diminishes with enlarging the number of scintillators participating in the software trigger. However, the speed of the decrease of events significantly differs for the EAS and TGE classes. In Fig. 6, we can see that the

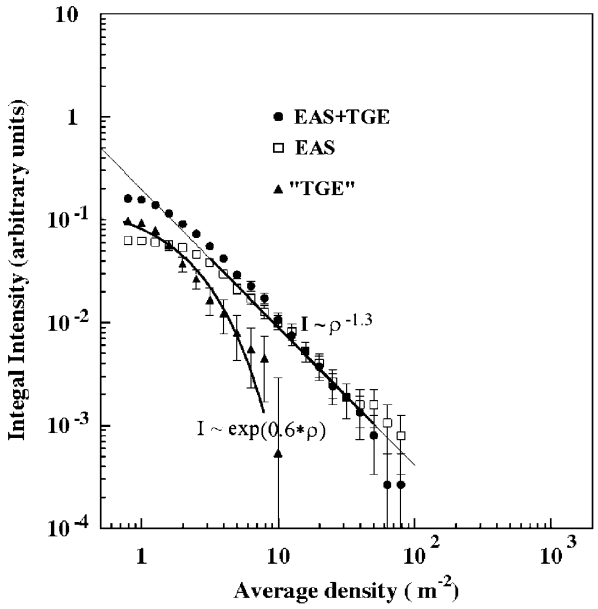

FIG. 5. Integral density distribution of the events from the joint TGE + EAS, statistically reconstructed TGE, and pure EAS classes.

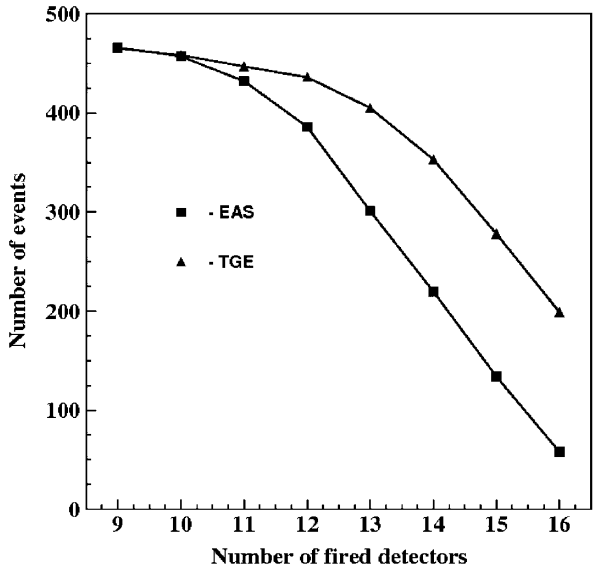

FIG. 6. Numbers of events detected with 9–16 scintillators of the Maket array for the two classes of events, both containing 465 events at hardware trigger conditions (9 scintillators fired).

number of EAS events is fast decreasing (from 465 at the trigger to 50 when all 16 scintillators are required). This can be explained by the small sizes of the EASs at rather low Maket array threshold energies ~50 TeV. The number of events of the TGE class is decreasing much slower. There are two possible reasons for the detected decrease in the number of events: the smaller than array dimension size of the event and the non-100% efficiency of the scintillators. We model the second possibility with 90% scintillator efficiency to register a charged particle.[6] Obtained trigger frequencies rather well coincide with the binomial law assuming a probability of success of 0.9. Therefore, we can state that there is no experimental evidence that the spatial elongation of the TGE events is less than 1000 m^2 (limit caused by the finite size of the Maket detector). Most of the EAS events are more compact.

IV. ESTIMATION OF THE MAXIMAL DURATION OF THE SHORT TGE EVENTS

The duration of the TGF events detected by gamma observatories on board low elevation satellites varies from several tens of microseconds to a few milliseconds, with a mean value of ~0.5 ms. At the present time we did not install megahertz flash amplitude-to-digital converters to measure the duration of the short TGE events directly; however, we establish the limits on the duration of the surface events by statistical analysis of the TGE event temporal distribution. The maximal duration of the surface particle bursts was estimated by exploiting the measured distribution of the TGE events in each of the seconds within a minute of the maximal flux (124 triggers at 22:47, 19 September, 2009). The data acquisition (DAQ) electronics and software operates as described below (see details in [16]):

(i) The Maket trigger system opens the window of ~1 μs after receiving the signal above the discriminator level from each of 16 channels.
(ii) If trigger conditions are fulfilled (8 selected +1 arbitrary scintillators are fired), 16 energy deposits are written in the temporary memory of the filled programmable gate arrays.
(iii) The duration of operations 1 and 2 is at most 50 μs, and it is the dead time of the Maket DAQ system.
(iv) The events (strings of 16 energy deposits) are collected during a second and then are transferred to permanent memory in an on-line ADAS personal computer.[7] Each event has a time stamp reporting when it was written in the temporary mass storage.
(v) ADAS joins the events collected in 1 s and transforms them to a 1-minute time series, storing them along with other information for sending to an MSQL database, where the ASEC time series are permanently stored.
(vi) If the duration of the event will exceed 50 μs after finishing of the dead time, another event will be generated and stored.

In Fig. 7, we present the distribution of the TGE triggers for the 3 selected minutes according to how many triggers were detected in a second. If, say, there is continuous detection of particles (discharge between a thundercloud and the ground) during a second, we can detect ~20 000 triggers (because of the 50 μs dead time of the DAQ electronics). If the TGE events have a duration exceeding the dead time of the detector, then several events will be detected within the same second; i.e. the detected events will be highly correlated and a very large number of events will fall in the particular second. However, even for the minute when the largest count rate occurred, at most 6 triggers per second were registered. It gives us a hint that the burst events are not correlated; however, we have to prove it formally by using the Neyman-Pearson technique of statistical hypothesis testing. As is usual in statistical hypothesis testing, we have to formulate the null hypothesis (H_0). It must be numerically exact—if it is valid, the distribution of the experiment outcomes (the distribution of the number of bursts in a second) should have a very definite shape close (within statistical errors) to the well known analytic distribution, thus allowing us to calculate the measure of the difference. If the calculated difference is

[6]Because of the aging of the scintillators (they have been in operation for ~20 years), the assumed efficiency is a realistic estimate.

[7]The Advanced Data Analysis System (ADAS) is a special software developed for on-line analysis and storing data from ASEC particle detectors; see details in [15].

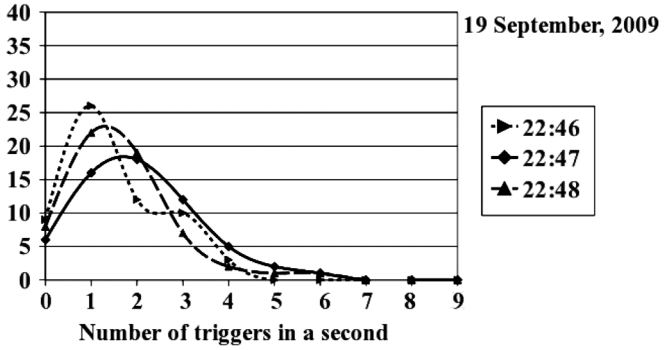

FIG. 7. Distribution of the Maket hardware triggers by the number of triggers per second at 3 minutes of 19 September, 2009.

greater than the preselected threshold value, we can state that the experimental results do not support H_0 and reject it (H_0 is rejected only for a first kind error—reject H_0 when it is true—is very unlikely). If the experimental distribution is close to the theoretical one, we accept H_0 stating that there is no evidence to reject it. Therefore, we formulate H_0 in the following way:

H_0 = there is no correlation between particle bursts measured by the Maket surface array.

The alternative hypothesis consists in the statement that particle bursts are correlated.

As we will see below, if H_0 is valid, we can numerically calculate the probabilities of having 1, 2, 3... bursts in a second using binomial, multinomial, and χ^2 analytical distributions. It is why we did not invert our procedure of the hypothesis testing and do not accept as H_0 the alternative hypothesis (bursts correlated). It will be very difficult (if even possible) to find the analytical distributions for arbitrary correlation of the bursts (TGEs).

The statistical hypothesis we have testing, the H_0 hypothesis (no correlation), consisted in several substatements. The distribution of the number of TGEs in a second can be described by the binomial distribution:

$P(X = r) = C^n{}_r p^r (1\text{-}p)^{n-r}$, where the combinatorial coefficient is $C^n{}_r = (n!/(n\text{-}r)!)/r!$.

The binomial model is valid when there are exactly two mutually exclusive outcomes of a trial. These outcomes are appropriately labeled success (TGE occurs in the selected second) and failure (TGE occurs during one of the other 59 seconds). The binomial distribution is used to obtain the probability of observing **r** successes in **n** trials, with the probability of success on a single trial denoted by **p** (in our case, $\mathbf{p} = 1/60$). The most important assumption of the binomial statistical model is the independent and identically distributed assumption: Trials (outcomes) of the experiment (TGEs) are independent, identically distributed variables, i.e. the assumption of no correlation between TGEs. To check this assumption we first will calculate binomial probabilities with a Web calculator [17] for the minute 22:47, 19 September, 2010; see column 3 in Table I.

For each minute we have a string of numbers. At the minute 22:47 of 19 September, 2009, we have, from 60 seconds, 6 seconds with no TGEs, 16 seconds with 1 TGF, 18 seconds with 2 TGFs, etc. To deal with the statistical experiment producing not only 2 outcomes as the binomial model but several outcomes, we have to adopt another statistical model, i.e. a multinomial model that has the following properties:

(i) The model consists of n repeated trials.
(ii) Each trial has a discrete number of possible outcomes (0 TGEs in a second, 1 TGE in a second, 2 TGEs in a second, ..., 124 TGE in a second).
(iii) On any given trial, the probability that a particular outcome will occur is constant.
(iv) The trials are independent; that is, the outcome of any of the trials does not affect the outcome of other trials.

To check the validity of the multinomial model, we have to compare the numbers of the experimentally obtained frequencies (column 3 of Table I) and expected frequencies calculated by binomial low (column 4 of Table I).

TABLE I. Comparison of the multinomial (H_0), simulated, and measured frequencies.

N of TGEs	Binomial probability $-\pi_i$	Experimental frequency at 22:47 (x_i)	Theoretical frequency $E_i = \pi_i * 60$	$(x_i - E_i)^2/E_i$	Simulated averaged frequency if TGE < 50 μs
0	0.124	6	7	1/7	7.5
1	0.261	16	16	0	15.8
2	0.273	18	17	1/17	16.2
3	0.188	12	11	1/11	11
4	0.096	5	6	1/6	5.6
5	0.039	2	2	0	2.3
6	0.013	1	1	0	1.4
>6	0.004	0	0	0	0.3
Sum	1.0	60	60	0.46	59.7

The validity of the null hypothesis was tested by using Pearson's chi-square test

$$\chi^2 = \sum_{i=1}^{k} \frac{(x_i - E_i)^2}{E_i},$$

where $E_i = N\pi_i$, $N = 60$, is the expected theoretical frequency. The normalized sum of deviations converges to a chi-square distribution with $k - 1$ degrees of freedom when the null hypothesis is true. From Table I we estimate the Pearson's χ^2 test value of 0.46 for 6 degrees of freedom. The corresponding chance probability of H_0 being false we can get from another Web calculator [18]. The chance probability of H_0 being false is 0.2% only; therefore, we do not have enough evidence to reject H_0, and we have to accept it; i.e. the particle bursts detected at 22:47, 19 September, 2010, are independent and identically distributed. From the physical analysis point of view it means that the TGE duration does not exceed 50 μs. We perform also a Monte Carlo study of the problem, generating trials of the short burst with durations less than 50 μs, greater than 50 μs, and less than 100 μs. If the duration of TGE events is greater than 50 μs and less than 100 μs, we can detect only even numbers of TGEs per second: 2, 4, 6, . . . And, of course, the χ^2 test will rocket to very high values, thus signaling that events are correlated. Obtained frequencies (averaged by 100 independent trials) are posted in the last column of Table I. Frequencies are in very good agreement with analytical calculations proving the independence of the TGE events with the confidence level 99%. Frequencies of the greater than 50 μs and less than 100 μs trials do not agree with both experimental and analytically obtained frequencies.

V. THE ELECTRICAL FIELD STRUCTURE DURING TGE EVENT ON 4 OCTOBER

The static electric field between the thunderclouds and the ground was measured with the Boltek EFM-100 electrical mill installed on Aragats research station at altitude 3250 m just on the Maket building where particle detectors are located. The electrical field measurements were taken 2 times in a second. In Fig. 8, we see the disturbance of the electrical field at Aragats station during the thunderstorm on 4 October, 18:00–18:40 UT. After a period of ~10 minutes of a large positive electrical field (~30 kV/m), the electrical field changed polarity and during another ~10 minutes reached values of about −30 kV/m (right vertical axes). The large negative field was accompanied by a huge flux of particles measured by the ASEC detectors [the 250% enhancement of the Maket triggers, left vertical axes; see, for details, Fig. 2(c)]. The zoomed pattern of the 2 minutes of the maximal flux, namely, 18:22—18: 24, is shown in Fig. 9 along with gamma-ray time series measured by the 01 combination of the ASNT (10 second time series) and lightning occurrence times.

In Fig. 9, we can see the correlations of electrical field, particle flux, and lightning occurrence in much more detail compared with the 1 minute time series. The decreasing of the electrical field is strongly correlated with the rising gamma-ray flux. Flux is reaching the maximal values near the maximum of the absolute value of the negative electrical field.

By the rectangles the intracloud-lightning occurrence time is denoted, measured by the Boltec storm tracker located on the Maket building. All lightnings within a radii of 5 km around the Maket building are depicted in Fig. 9.

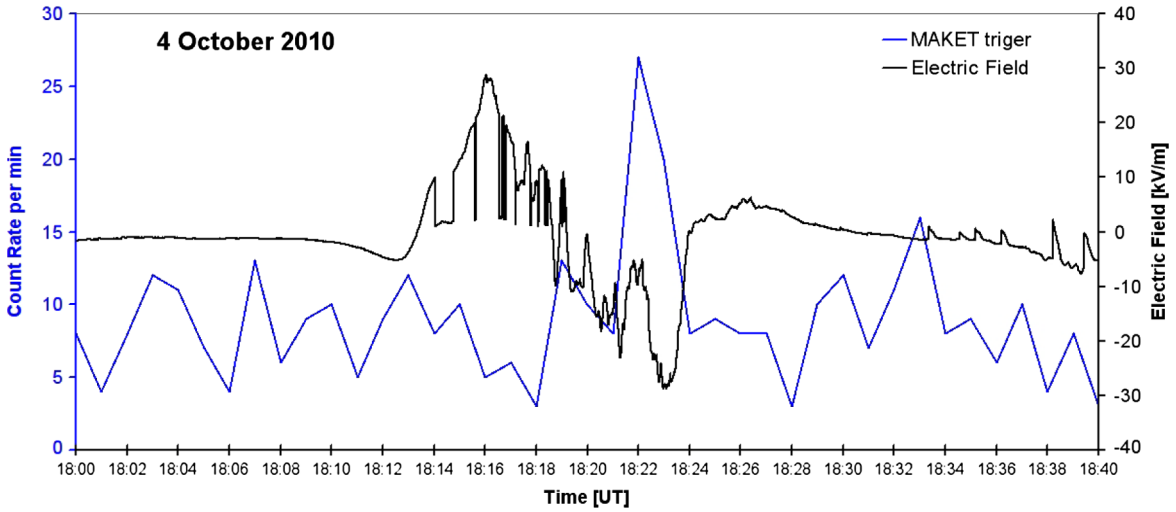

FIG. 8 (color online). The temporal structure of the electrical field disturbances and the time series of the Maket triggers detected on 4 October, 2010.

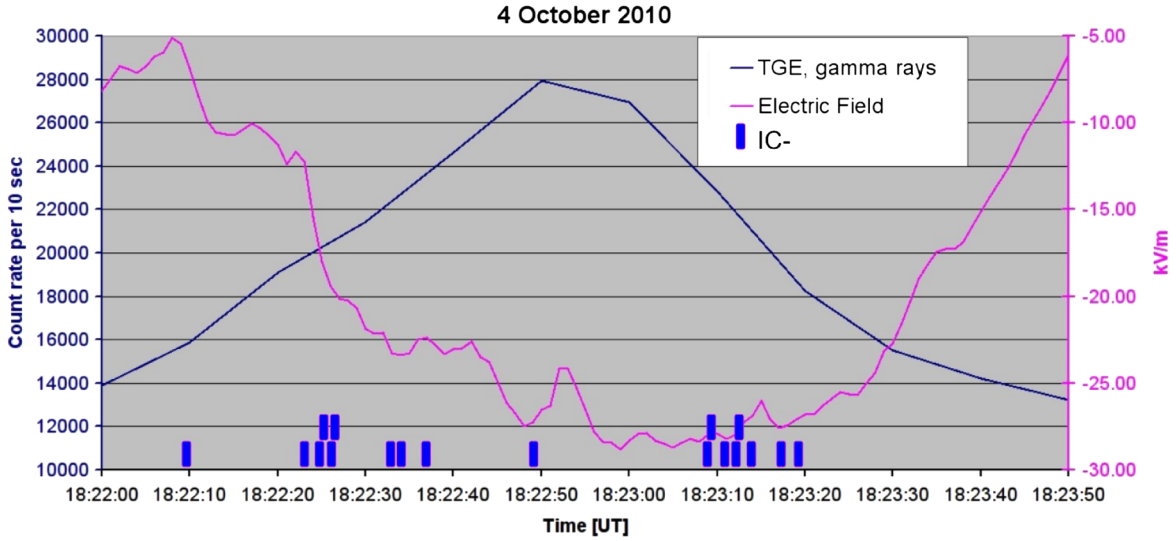

FIG. 9 (color online). Disturbed electric field and count rate of the gamma rays (energy >10 MeV) measured by the 01 combination of the Aragats Solar Neutron Telescope: 4 October, 2010, 18:22–18:24.

Remarkably, only 18 negative intracloud lightnings were detected during the maximal flux of the TGE, no intracloud positive, and no cloud-ground lightning was detected.

VI. DISCUSSION

We report the new observed phenomenon of the short TGEs (duration less than 50 μs) detected by the surface particle detectors at mountain altitudes. Short particle bursts occur during a large negative electrical field measured between cloud and the ground accompanied by numerous negative intracloud lightnings. In two episodes on September 19, 2009, and October 4, 2010, lasting totally 10 minutes, $(8 + 2) \sim 340$ short TGE events were detected. Observed short TGEs, in contrast to prolonged ones (described in detail in our previous paper, Ref. [11]) can be compared with TGFs routinely detected by orbiting gamma-ray observatories [3,5].

(i) The origin of the TGFs was estimated to be in (or just above) thunderclouds in the upper troposphere and lower stratosphere, at altitudes 15–21 km [19,20].

(ii) The mean duration of a TGF is ~500 μs and mean fluence ~1 particle/cm^2 [Ramaty High Energy Solar Spectroscopic Imager (RHESSI) observations].

(iii) Maximal energy—up to 50 MeV by Fermi [2] and AGILE observations [4] and even 100 MeV [21].

(iv) Cummer *et al.* [22] based on a subsample of RHESSI TGFs establish TGF correlation with lightning discharges: 50% of analyzed 26 TGFs are found to occur within $-3/+1$ ms of the positive intracloud (+ IC) lightning discharges inside a ~300 km radii circle around the RHESSI subspacecraft position.

(v) Fermi gamma burst monitor data [23] confirm this finding, establishing an association of the 15 from a total of 50 TGFs with individual discharges. Surprisingly, both associations did not establish the time order of lightning-TGF occurrence.[8]

The observed rich phenomenology of the TGFs shortly presented above poses rather stringent constraints on the physical process responsible for TGF generation. According to analysis in [8,20] the huge upward ($\sim 10^{17}$) flux of the gamma rays is responsible for the observed TGFs. A sufficient amount of the seed electrons necessary for the production of 10^{17} gamma rays by the RREA developing (see Fig. 10) is provided by the streamers and stepped lightning leaders [8–10] in the intracloud positive lightning (+ IC [20]; see Fig. 10). The proposed mechanism also naturally supported the harmony of the time scales of the electron emission and TGF duration (see Table 2 in [8]).

Downward development of the RREA requires a positive electrical field in the cloud and, therefore, a negative field between clouds and the ground (see Fig. 10). The posed limit on the event maximal duration of 50 μs also puts severe restrictions on the physical mechanism responsible for the short TGEs. And again stepped leader propagation fits best to submit seed particles in the time scale adequate to the short TGEs. Consequently, the negative intracloud lightning (− IC) could provide seed particles for the TGEs detected by the Maket detector. As we can see in Fig. 9, the measured electrical field and observed negative intracloud lightnings support the model depicted in Fig. 10.

Thus, the generation mechanisms of the space TGFs and short TGEs are close to each other and symmetric: *RREA*

[8]The estimated mean delay of the RHESSI TGFs relative to lightning is −1.24 ms [22].

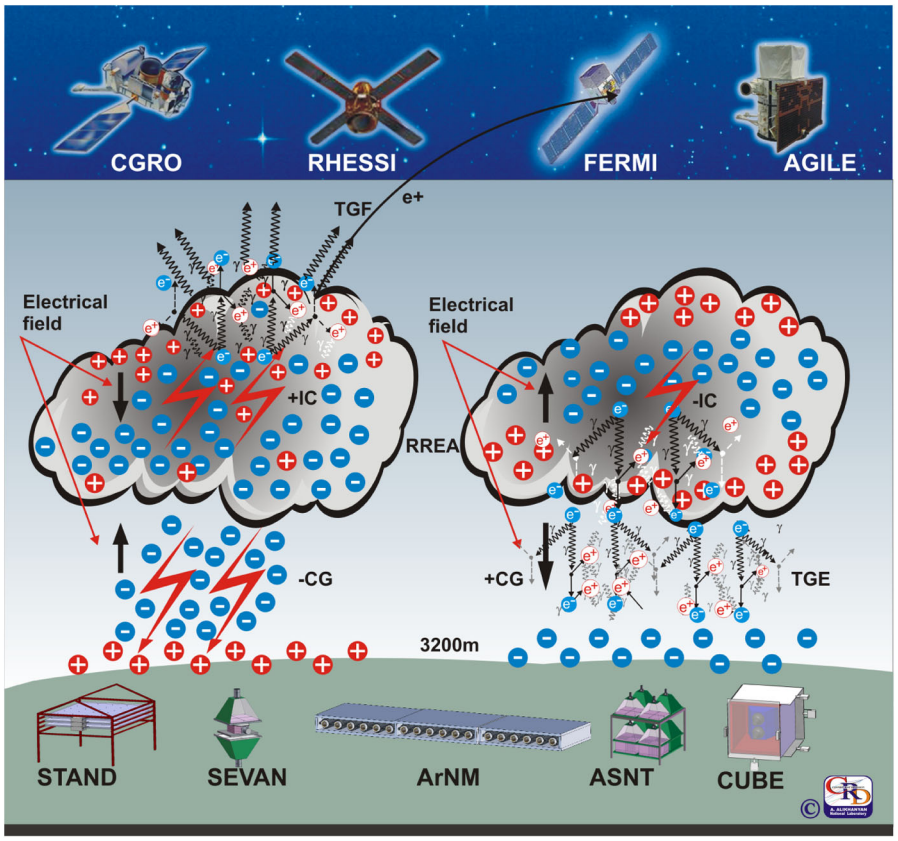

FIG. 10 (color online). Symmetry of the TGFs and TGEs.

uses as the seeds the electrons from the current pulses along the step leaders ($\pm$ IC) *and developing in consequent negative and positive electrical fields.*

Seed electrons for the long TGEs are provided by the ambient population of MeV electrons from the secondary cosmic rays. As we show in [11] the population of the secondary electrons from the particle showers initiated by the primary hadron entering the terrestrial atmosphere is sufficient to generate via the RREA process enough particles to explain the huge surface enhancement on 19 September, 2010.

However, there are significant differences in TGE and TGF events.

(i) Short TGEs are very rare events (detected at Aragats about once a year); the Maket array observes the sky just above the detector ($\sim 10^6$ m^2). Fermi and AGILE are observing huge areas reaching $\sim 10^{12}$ m^2; therefore, the number of detected TGFs is much larger, reaching hundreds per year.

(ii) Nonetheless, because of the closeness of the particle beam, the number of detected TGEs in 2 series of detection is rather large: $\sim$325. TGE develops in a rather dense atmosphere; only the close location of the thundercloud to the ground and rather large elongation of the strong electrical field in the thundercloud can provide unique possibilities of detection of TGE electrons and gamma rays (see details in [11]).

(iii) The duration of the TGE is more than an order of magnitude shorter than the ones of TGF. Gamma rays arriving at satellite altitude are covering at least 3 orders of magnitude longer path length compared to TGEs and arrive spread over a pulse of $\sim$500 μs. TGEs come from thunderclouds just above our heads and cover less than 500 m; therefore, they come in pulses with a duration less than 50 μs.

VII. CONCLUSION

We discover new energetic atmospheric phenomena, namely, short TGEs tightly connected with the ones detected by orbiting gamma-ray observatories, i.e. TGFs. The basis of high-energy emissions from the thunderstorm atmospheres is believed to be large electrostatic fields within thunderclouds, the mechanism—RREA); seed particles—ambient population of MeV electrons from EAS (for long TGEs) and electrons from current pulses of step leaders of intracloud lightning.

ACKNOWLEDGMENTS

This work was partly supported by the Armenian government grants and by ISTC Grant No. A1554.

The authors are grateful to participants of the conference TEPA-2010 and to members of the seminar of the cosmic-ray division of Alikhanyan national lab for useful discussion.

APPENDIX: DISCUSSION ON THE POSSIBILITY OF INTERFERENCES AND ELECTRONIC OR NATURAL INDUCED SIGNALS TO GENERATE PEAKS IN TIME SERIES OF THE ASEC PARTICLE DETECTORS

There are numerous sources of natural and electronics emissions that can mimic the peaks in the time series of particle detector count rates. To answer if the peaks apparent in the time series of the ASEC particle detectors during thunderstorms can be fake, we performed an in-depth analysis of the enhancements of the ASEC detectors and collected evidence demonstrating the existence of the indisputable additional particle fluxes responsible for the detected peaks.

400 m apart at Aragats are in operation same type detectors (AMMM—Aragats Multichannel Muon Monitor—and Maket) with fully independent cabling and DAQ electronics demonstrate similar time-coherent peaks (see Fig. 11).

The enhancements detected by the ASNT are concentrated only in the region of the small energy deposits; the large energy deposits remain unchanged (see Fig. 12).

The ASNT detector measures the incoming directions of the detected particles. The count rates of the near vertical and inclined particles are dramatically different. If we observe huge enhancement in the near vertical direction (expected arrival direction of the RREA particles), at the same time on the same detector using the same DAQ electronics and analysis software we measure a deficit in the inclined particle flux (maybe due to stopping positive muons; see Fig. 13).

The SEVAN particle detector measured 3 types of particle fluxes: low-energy charged particles, neutral particles, and high-energy particles (above 250 MeV, mostly muons). In Fig. 14, we can see a deficit of high-energy muons ($E_\mu > 250$ MeV) and a huge peak in the time series of neutral particles (there is also a peak in the time series of the low-energy charged particles). All 3 types of particle fluxes are detected by the SEVAN detector with one and the same cabling and DAQ electronics.

Nonetheless, we detect some induced signals in a few from hundreds of the ASEC detectors due to radio emission of the lightning. Lightning is a powerful broadband radio signals emitter. The pulse power of the radio signals can reach 100 GW. And if the detector is poorly grounded, or some of the cables have bad isolation, the radio signals induced peaks in these channels. We systematically monitor and repair failure equipment. However, lightning-induced signals in the poorly grounded counters have a very specific shape and follow the pattern of the lightning activity, now also monitored by the ASEC facilities. Therefore, it is not very difficult to outline fake peaks and repair the malfunctioning channels.

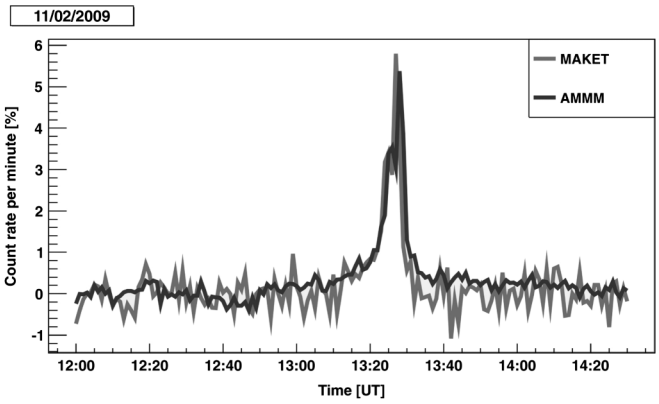

FIG. 11. Time series of the AMMM outdoor 5 cm scintillator and the Maket outdoor 5 cm scintillators located at a distance of 400 m from AMMM; TGE on 2 November, 2009.

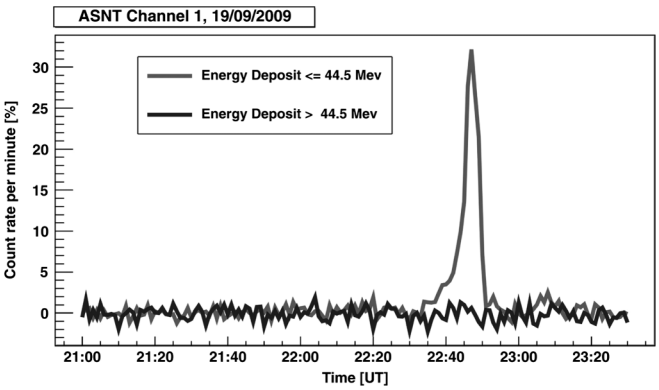

FIG. 12. Time series of the ASNT corresponding to different energy releases during TGE on 19 September, 2009.

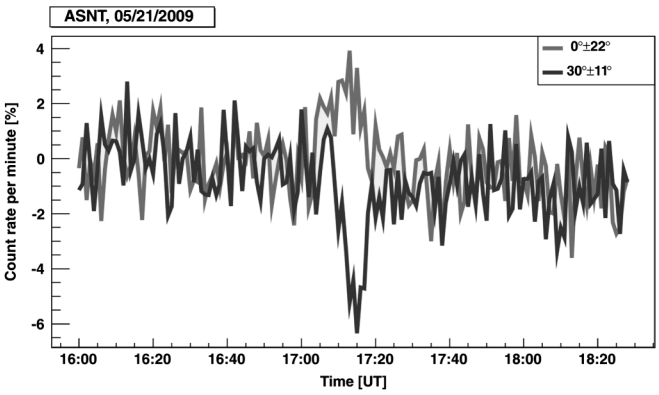

FIG. 13. Time series of ASNT corresponding to different directions of the incoming particle flux; TGE on 21 May, 2009.

[1] J. R. Dwyer, B. W. Grefenstette, and D. M. Smith, Geophys. Res. Lett. **32**, L22804 (2005).
[2] M. S. Brigs *et al.*, J. Geophys. Res. **115**, A07323 (2010).
[3] G. J. Fishman *et al.*, Science **264**, 1313 (1994).
[4] M. Marisaldi *et al.*, J. Geophys. Res. **115**, A00E13 (2010).
[5] D. M. Smith *et al.*, Science **307**, 1085 (2005).
[6] A. V. Gurevich, G. M. Milikh, and R. A. Roussel-Dupre, Phys. Lett. A **165**, 463 (1992); A. V. Gurevich *et al.*, Phys. Lett. A **373**, 3550 (2009).
[7] C. T. R. Wilson, Proc. Cambridge Philos. Soc. **22**, 534 (1925).
[8] B. E. Carlson, N. G. Lehtinen, and U. S. Inan, J. Geophys. Res. **114**, A00E08 (2009).
[9] G. D. Moss, V. P. Pasko, N. Liu, and G. Veronis, J. Geophys. Res. **111**, A02307 (2006).
[10] Z. Saleh, J. Dwyer, J. Howard, M. Uman, M. Bakhtiari, D. Concha, M. Stapleton, D. Hill, C. Biagi, and H. Rassoul, J. Geophys. Res. **114**, D17210 (2009).
[11] A. Chilingarian *et al.*, Phys. Rev. D **82**, 043009 (2010).
[12] N. S. Khaerdinov, A. S. Lidvasky, and V. B. Petkov, Atmos. Res. **76**, 346 (2005).
[13] A. Chilingarian *et al.*, J. Phys. G **29**, 939 (2003).
[14] A. Chilingarian *et al.*, Nucl. Instrum. Methods Phys. Res., Sect. A **543**, 483 (2005).
[15] A. Chilingarian *et al.*, Astropart. Phys. **28**, 58 (2007).
[16] K. Arakelyan *et al.*, in *Proceedings of the Third International Conference Solar Extreme Events, National & Kapodistrian University of Athens, Greece* (National & Kapodistrian University of Athens, Athens, 2009), pp. 363–367.
[17] http://stattrek.com/Tables/Binomial.aspx.
[18] http://www.physics.csbsju.edu/stats/chi-square_form.html.
[19] J. R. Dwyer, B. W. Grefenstette, and D. M. Smith, Geophys. Res. Lett. **35**, L02815 (2008).
[20] E. Williams *et al.*, J. Geophys. Res. **111**, D16209 (2006).
[21] M. Tavani *et al.*, Phys. Rev. Lett. **106**, 018501 (2011).
[22] S. A. Cummer, Y. Zhai, W. Hu, D. M. Smith, L. I. Lopez, and M. A. Stanley, Geophys. Res. Lett. **32**, L08811 (2005).
[23] V. Connaughton *et al.*, J. Geophys. Res. **115**, A12307 (2010).